Energetics and electronic structure of aluminum point defects in HfO_2: A first-principles study

Z. F. Hou,[1] X. G. Gong,[1,a)] and Quan Li[2]
[1]*Department of Physics and Surface Physics Laboratory, Fudan University, Shanghai 200433, People's Republic of China*
[2]*Department of Physics, The Chinese University of Hong Kong, Shatin, New Territory, Hong Kong*

(Received 10 September 2008; accepted 28 February 2009; published online 7 July 2009)

Using the plane-wave pseudopotential method within the generalized gradient approximation, we studied the atomic structure, energetics, and electronic structure of the interstitial and substitutional point defect of dopant aluminum in monoclinic HfO_2. Our results show that the doped Al atom energetically prefers to substitute for the Hf atom under the oxygen-rich condition. Substitution of Al for Hf creates a shallow acceptor level near the valence band maximum, whereas both substitution of Al for O and interstitial Al introduce deep levels in the band gap of HfO_2. We also discussed the possible effect of Al doping on the electronic properties of HfO_2.
 [DOI: 10.1063/1.3109206]

I. INTRODUCTION

Hafnia (HfO_2) is a wide-band-gap oxide with a relatively high dielectric constant and electron barriers.[1] Recently, HfO_2 received much attention among gate-dielectric materials of metal-oxide-semiconductor devices due to its potential application as alternative to SiO_2.[1,2] However, pure as-deposited amorphous HfO_2 is easy to crystallize during post-deposition annealing (for example ~400 °C) (Ref. 3) and may induce nonuniformity of the film thickness.[2] Considering that Al_2O_3 is known to act as an oxygen diffusion barrier and also as a good glass constituent, it is expected to improve the thermal stability of HfO_2 by adding Al_2O_3 as dopant, which was demonstrated in recent experiments that Hf aluminate films are thermally stable and remain amorphous up to 900 °C.[3–5]

Charge trapping, a common phenomenon observed in most high-κ metal oxides, is believed to happen due to existing defects in the high-κ oxides layer and/or its interfaces with silicon.[6] Therefore, the related defects have been the subject of intensive experimental and theoretical studies for high-κ gate oxide stacks. Recent studies suggest that addition of Al into HfO_2 could passivate the defect states of positively charged oxygen vacancies[7] and reduce the total trap density.[8] However previous experimental study[5] reported that doping Al into HfO_2 introduces fixed negative charges, which results in mobility degradation, due to Al accumulation at the HfAlO–Si interface. Since the band gap of Al_2O_3 is much larger than that of HfO_2, it is expected that alloying HfO_2 with Al_2O_3 could enlarge the band gap of HfO_2 and the conduction band offsets of HfO_2 with respect to silicon.[4] In order to understand the effect of Al doping on the electronic structures of HfO_2 dielectric film, it is hence important to study Al point defects in HfO_2 at the atomic scale.

In this study, the plane wave pseudopotential method is employed to investigate the defect formation energies and electronic structures of interstitial and substitutional point defects of the doped Al atom in the monoclinic phase HfO_2 (m-HfO_2). We also discuss the possible behavior of Al doping and its effect on the electronic structures of HfO_2.

II. COMPUTATIONAL METHODS

All calculations were performed by means of the plane-wave pseudopotential method, as implemented in the Vienna *ab initio* simulation package (VASP).[9,10] The exchange and correlation potential is treated by means of the generalized gradient approximation (GGA) with Perdew and Wang parametrization (known as GGA-PW91).[11] The ultrasoft pseudopotentials[12,13] implemented in VASP are used to represent the electron-ion interaction. The pseudopotential was generated with respect to the valence electron configuration $5d^3 6s^1$ for hafnium atom, $2s^2 2p^4$ for oxygen atom, and $3s^2 3p^1$ for aluminum atom. The crystal wave function is expanded by the plane waves up to an energy cutoff (E_{cut}) of 500 eV. Numerical integrations over Brillouin zone (BZ) are done by the special k-points sampling.

To check the applicability and accuracy of the above pseudopotentials, calculations on oxygen molecule, hcp hafnium, fcc aluminum, m-HfO_2, and rhombohedral alumina (α-Al_2O_3) were carried out. For the calculation on O_2, an isolated O_2 molecule was placed in a cubic cell with the dimension of $15\times15\times15$ Å^3 and only the Γ point was used. For the calculations on hcp Hf, fcc Al, m-HfO_2, and α-Al_2O_3, the special k-points sampling in BZ was generated by the Monhkorst–Pack scheme[14] with k-point grids of $9\times9\times5$, $11\times11\times11$, $5\times5\times5$, and $9\times9\times9$, respectively. All the total energies of the above molecule and bulk systems are converged within tenths of meV, with respect to above choice of E_{cut} and k-point grid sizes. A full optimization of the atomic positions in the unit cell and the lattice parameters was performed for all the studied bulk systems. The adopted convergence criteria for the force exerting on each atom and the stress in the lattice are less than 0.01 eV/Å and 0.1 GPa, respectively. The same convergence criteria for the force exerting on an atom was also adopted for the atomic relaxation

a)Electronic mail: xggong@fudan.edu.cn.

TABLE I. Calculated bond length (d_{O-O}, in angstroms) of the O_2 molecule and lattice parameters (in angstroms) of hcp Hf, fcc Al, m-HfO_2, and α-Al_2O_3 in rhombohedral primitive cell, along a comparison with previous theoretical results and available experimental values. x, y, and z are the fractional coordinates of the nonequivalent sites and β (in degrees) is the angle between primitive vectors $\vec{a}$ and $\vec{c}$ of the monoclinic cell of HfO_2. θ (in degrees) is the angle between primitive vectors of the rhombohedral primitive cell of α-Al_2O_3 and u_{Al}/v_O for the internal coordinate parameters of Al/O atoms.

	Calculated		
Property	Present	Previous	Experimental
		O_2 molecule	
d_{O-O}	1.24	1.24[a]	1.21[b]
		hcp Hf	
a, c	3.179, 5.023	3.180, 5.024[c]	3.195, 5.051[d]
		fcc Al	
a	4.04	4.04[a]	4.05[d]
		m-HfO_2	
a, b, c	5.133, 5.188, 5.301,	5.132, 5.189, 5.307[c]	5.119, 5.170, 5.298[e]
β	99.79	99.78	99.18
Hf(x,y,z)	(0.276, 0.043, 0.207)	(0.277, 0.044, 0.209)	(0.276, 0.040, 0.207)
O1(x,y,z)	(0.070, 0.334, 0.343)	(0.070, 0.333, 0.345)	(0.071, 0.332, 0.344)
O2(x,y,z)	(0.448, 0.758, 0.479)	(0.448, 0.758, 0.478)	(0.446, 0.755, 0.480)
		α-Al_2O_3	
a	5.196	5.195[a]	5.128[f]
θ	55.32	55.32	55.20
u_{Al}	0.353	0.352	0.352
v_O	0.556	0.556	0.556

[a]Reference 23.
[b]Reference 20.
[c]Reference 18.
[d]Reference 21.
[e]References 15–17.
[f]Reference 22.

of oxygen molecule. The optimized bond length of O_2 and structural parameters of these metals and oxides are listed in Table I. Especially for monoclinic phase of HfO_2, the obtained lattice parameters are a=5.133 Å, b=5.188 Å, c=5.301 Å, and β=99.79°, in good agreement with the experimental values (a=5.199 Å, b=5.170 Å, c=5.298 Å, and β=99.18°)[15–17] and other GGA calculation results.[18,19] The formation energies (ΔE_f) of m-HfO_2 and α-Al_2O_3 are calculated by the following equation:

$$\Delta E_f = \begin{cases} E_{tot}(HfO_2) - \mu^0_{Hf} - 2\mu^0_O & \text{for } HfO_2 \\ E_{tot}(Al_2O_3) - 2\mu^0_{Al} - 3\mu^0_O & \text{for } Al_2O_3 \end{cases}, \quad (1)$$

where $E_{tot}(HfO_2)$ and $E_{tot}(Al_2O_3)$ are the total energies per formula unit (f.u.) of m-HfO_2 and α-Al_2O_3, respectively. μ^0_{Hf}, μ^0_O, and μ^0_{Al} are taken as the total energies per atom of hcp Hf, an oxygen molecule, and fcc Al, respectively. The calculated formation energy of m-HfO_2 is −10.92 eV/HfO_2 (see Table II), which agrees well with the previous theoretical value of −10.95 eV/HfO_2 from GGA calculations.[18] For oxygen molecule and other bulk systems calculated here, present results (see Tables I and II) are also in good agreement with the available experimental values[20–22] and previous theoretical calculation results.[18,23]

TABLE II. Calculated formation energies (ΔE_f, in eV/f.u.) for m-HfO_2 and α-Al_2O_3.

Constituents	Present	Previous	Experimental
$Hf+O_2 \rightarrow HfO_2$	−10.92	−10.95[a]	···
$2Al+(3/2)O_2 \rightarrow Al_2O_3$	−15.33	−16.71[b]	−17.37[c]

[a]Reference 18.
[b]Reference 23.
[c]Reference 20.

In order to study the possible behavior of Al doping in HfO_2, the doped Al atom occupying different positions in the lattice, such as interstitial position, substituting for a hafnium atom, and substituting for an oxygen atom (essentially an antisite configuration) are considered. HfO_2 supercells are constructed for Al point defects calculations. The supercell consisting of 96 atoms was generated by doubling the size of unit cell of the optimized monoclinic HfO_2 in three dimensions. Due to the large size of the supercell, single Γ point was employed for k-point sampling with an energy convergence of 9 meV/HfO_2. A neutralizing background was applied to the supercell in the calculations of Al point defects in different charge states. During the geometry relaxation, the basis vectors of the supercell were fixed and the force exerting on each atom is calculated to guide the movement of all atoms until the residual force was converged to be less than 0.01 eV/Å.

III. RESULTS AND DISCUSSIONS

Our calculations are performed in supercell with 96 atoms. Point defect of interstitial Al (denoted as Al_i) is modeled by putting an extra Al atom on the interstitial site around

TABLE III. Distances to nearest-neighbor atoms in bulk α-Al_2O_3, bulk m-HfO_2, and HfO_2 supercells containing neutral Al point defects. d_i (in angstoms) is the distance of the ith nearest neighbor.

Atom	System	Neighbor type	d_1	d_2	d_3
Al	α-Al_2O_3	O	1.88	2.00	⋯
Hf	m-HfO_2	O	2.04	2.06	2.14
Al	Al_i	O	1.78	1.81	1.94
		Hf	2.68	2.70	2.76
Al	Al_{Hf}	O	1.86	1.94	1.96
		Hf	3.10	3.30	3.41
Al	Al_O	O	1.81	1.92	2.31
		Hf	2.67	2.71	2.78

the threefold coordinated lattice oxygen atom, while point defect of substitutional Al is constructed by replacing one of the lattice atoms, Hf or O, with Al atom (denoted as Al_{Hf} or Al_O, correspondingly) in the HfO_2 supercells. We relaxed the atomic positions for each kind of point defect in the supercell. The nearest neighbor distances between the Al atom and the lattice atoms are listed in Table III. It can be seen that doping Al into HfO_2 host leads to large atomic relaxation. The lattice oxygen atoms around the Al atom move toward the Al atom, resulting in the bond length between Al and O atoms equal to or shorter than that in bulk α-Al_2O_3. This can be seen from the contour plots of charge density across the plane containing the Al impurity, lattice Hf, and lattice oxygen atoms, as shown in Fig. 1, which clearly demonstrates that the interaction between additional Al atom and lattice oxygen atom is stronger than the bonding between Hf and O atoms. This is consistent with experimental observation that HfO_2 can be stabilized by adding Al_2O_3 as a dopant to change the bonding characteristics.[24]

The calculated total energies as well as atomic chemical potentials are used to determine the formation energies of the studied point defect α in charge state q, according to the following formula:[25–27]

$$\Delta E_f(\alpha,q) = E(\alpha,q) - \sum_i N_i\mu_i + q(\varepsilon_F + E_{\mathrm{VBM}}), \tag{2}$$

where $E(\alpha,q)$ is the total energy of the defective supercell containing N_i atoms of species i with chemical potential μ_i. The Fermi level ε_F is measured relative to the valence band maximum (VBM), E_{VBM}. Because the potential with periodic boundary conditions can only be determined up to a constant, in order to accurately determine E_{VBM}, it is necessary to line up the potentials of the perfect and defective supercells. For this purpose, we align the average potential at a position far away from the defect in the defective supercell with that in the perfect supercell.[28] In the case of Al point defects in HfO_2 supercells, Eq. (2) can be rewritten in terms of the total energy of the perfect HfO_2 supercell (E_0^0) as

$$\Delta E_f(\alpha,q) = E(\alpha,q) - (E_0^0 + n_{\mathrm{Hf}}\mu_{\mathrm{Hf}} + n_{\mathrm{O}}\mu_{\mathrm{O}} + n_{\mathrm{Al}}\mu_{\mathrm{Al}}) + q(\varepsilon_F + E_{\mathrm{VBM}}), \tag{3}$$

where n_{Hf}, n_{O}, and n_{Al} are the number of Hf, O, and Al atoms removed from or added to the perfect supercell to introduce the substitutional or interstitial Al point defects. For example, (n_{Hf}, n_{Al}, and n_{O}) is taken as (−1, 1, 0) for a point defect of Al_{Hf}. In the present study, the charge states of Al point defects are taken as −1 or 0 for Al_{Hf}, and 0∼+3 for Al_i and Al_O. The ε_F is kept within the band gap,

$$0 \le \varepsilon_F \le E_g. \tag{4}$$

The band gap E_g can be obtained by the calculated band structure and density of states (DOS). The total and orbital projected DOS of m-HfO_2 are shown in Fig. 2. It can be seen that a valence band of oxygen $2p$ occurs just below VBM and a conduction band of hafnium $5d$ occurs above 3.80 eV. The major contribution to the states near the VBM comes from O $2p$ states with minor contribution from Hf p, d states, which is consistent with the picture of HfO_2 as an ionic insulator with bonds between Hf and O of some covalent component.[18,19] The calculated indirect band gap of monoclinic HfO_2 from Γ to B is 3.80 eV, which is lower than the experimental value of 5.68 eV,[15] but is consistent with other *ab initio* GGA calculations.[19] The underestimation of the band gap energy value is typical of density functional theory calculations in the GGA or local density approximation (LDA). The difference between the theoretical and experimental gap is the main source of inaccuracy for the defect levels. The chemical potentials, μ_{Al}, μ_{Hf}, and μ_{O}, depend on the doping conditions. For the chemical potentials of Hf and O, one limit was considered: under oxygen-rich condition, the μ_{Hf} is taken as $\mu_{\mathrm{Hf}}=\Delta E_f(HfO_2)+\mu_{\mathrm{Hf}}^0$ and μ_{O} as μ_{O}^0.[18,29] At the same time, we considered two limits for the chemical potential of Al: (i) μ_{Al} as the chemical potential of crystalline fcc Al, i.e., $\mu_{\mathrm{Al}}=\mu_{\mathrm{Al}}^0$, which would correspond to the extreme Al-rich doping condition and the formation of Al clusters in the bulk or at the surface of the oxide and (ii) μ_{Al} as the chemical potential of Al in α-Al_2O_3 corresponding to extreme oxygen-rich condition, i.e., $\mu_{\mathrm{Al}}=(1/2)\Delta E_f(Al_2O_3)+\mu_{\mathrm{Al}}^0$. In the first case of the chemical potential of Al, the

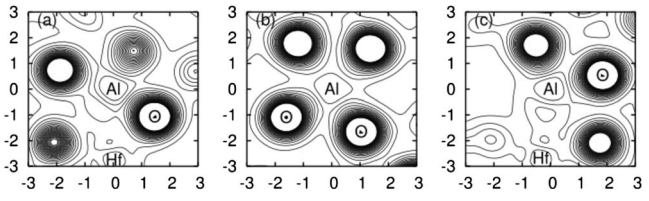

FIG. 1. Contour plots of charge density in the cross-sectional planes for (a) neutral Al_i, (b) neutral Al_{Hf}, and (c) neutral Al_O point defects at equilibrium in monoclinic HfO_2. Charge density is shown in an increment of 0.1 $e/Å^3$ from 0 to 2.1 $e/Å^3$ and distances in angstroms.

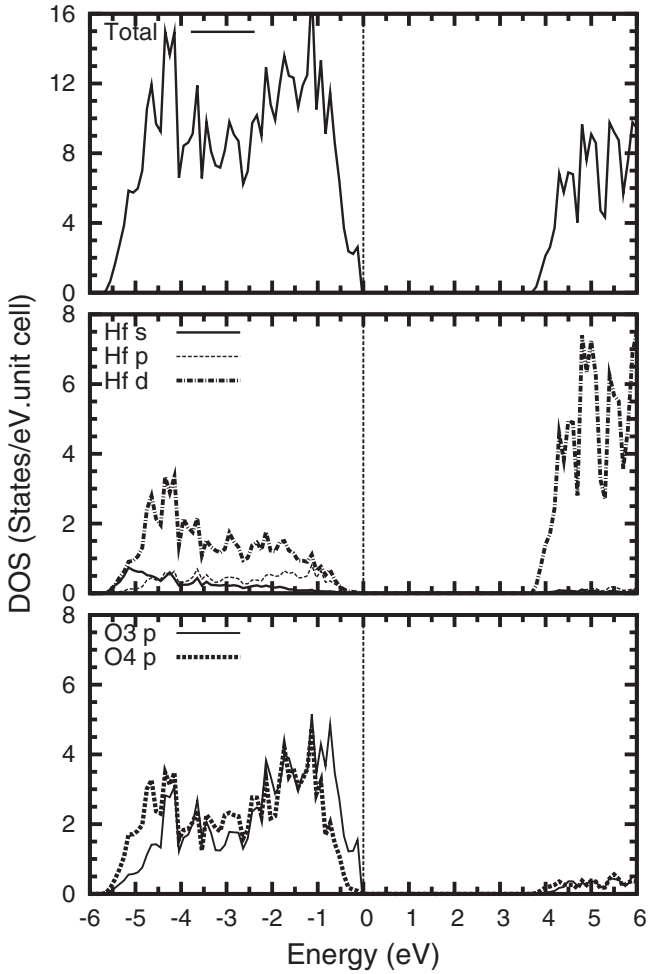

FIG. 2. Total and *lm*-projected DOS of monoclinic HfO_2. O3 stands for three-coordinated oxygen and O4 represents the four-coordinated one.

formation energies of neutral Al_i, Al_O, and Al_{Hf} point defects are 4.58, 9.84, and −5.78 eV, respectively. In the second case considered above, the formation energies of neutral point defects of Al_i, Al_O, and Al_{Hf} are 12.26, 17.52, and 1.87 eV, respectively. These indicate that under oxygen-rich condition the doped Al atom energetically prefers to substitute for Hf atom. In other words, substituting Al for Hf is very likely to occur under the oxygen-rich condition as in the following situations: heavy doping of Al, a small amount of Al_2O_3 is mixed with HfO_2 to form hafnium aluminate, or a thin layer of Al_2O_3 exists between the Si substrate and the HfO_2 film. These also suggest that the formation of HfAlO laminate would be thermodynamically favorable.

The formation energies versus the electronic chemical potential ε_F for the interstitial and substitutional Al point defects in a range of charge states are shown in Fig. 3. The lower limit of the Fermi level ($\varepsilon_F=0$ eV) corresponds to the top of the valence band while the upper limit ($\varepsilon_F=5.68$ eV) is the bottom of the experimental conduction band. The slope of the line in Fig. 3 corresponds to the charge state of point defect. The calculated formation energies of interstitial Al point defects in different charge states, as shown in Fig. 3, indicate interstitial Al is favorable in the fully ionized state, accompanied by a decay reaction of $Al_i^+ + Al_i^{2+} \Rightarrow Al_i^0 + Al_i^{3+}$ with a released energy of 0.54 eV. For

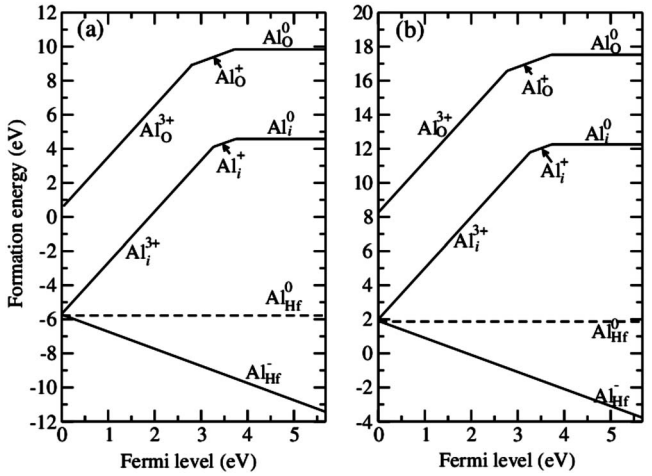

FIG. 3. Calculated formation energy vs Fermi level for the point defects of Al_i, Al_{Hf}, and Al_O in HfO_2. Two cases are considered for the chemical potential of Al: (a) μ_{Al} as the chemical potential of crystalline fcc Al, i.e., $\mu_{Al}=\mu_{Al}^0$ and (b)μ_{Al} as the chemical potential of Al in α-Al_2O_3 corresponding to extreme oxygen-rich condition, i.e., $\mu_{Al}=(1/2)\Delta E_f(Al_2O_3)+\mu_{Al}^0$. The oxygen-rich environment is considered for the chemical potentials of O and Hf: $\mu_O=\mu_O^0$ and $\mu_{Hf}=\Delta E_f(HfO_2)+\mu_{Hf}^0$.

substitutional Al on O site, the reaction $Al_O^0 + Al_O^{3+} \Rightarrow Al_O^+ + Al_O^{2+}$ gains an energy of 0.59 eV. In addition, substitutional Al on Hf site prefers a single negatively charged state for electronic chemical potential varying over the whole range from the lower limit to the upper one. Therefore, our results suggest that the introduced fixed negative charge in the HfAlO film with poly-Si gate reported in Ref. 5 may partially result from the substitution of Al for Hf.

Now we turn to discuss the defect levels induced in the band gap by Al point defects. The schematic of the single-electron energy levels in the calculated band gap of monoclinic HfO_2 for the point defects of interstitial and substitutional Al are shown in Fig. 4. It can be seen that the formation of neutral Al_i introduces a fully occupied defect state at 2.32 eV and a half-occupied defect level at 3.72 eV above the VBM. Analysis of the angular-momentum-projected DOS reveals that the first extra level at 2.32 eV

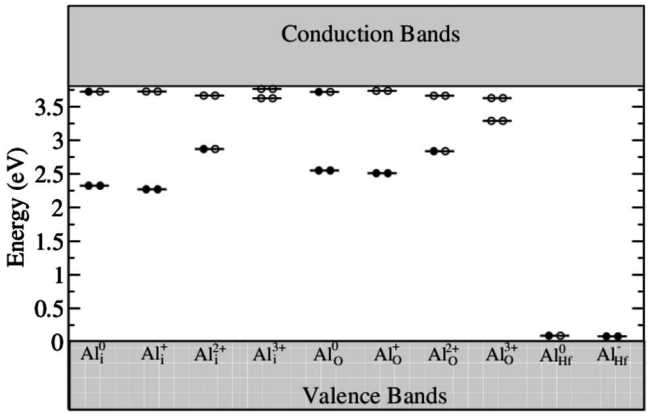

FIG. 4. Schematic of the single-electron energy levels induced in the calculated band gap of monoclinic HfO_2 by Al_i, Al_{Hf}, and Al_O point defects in different charge states. Solid and open dots stand for the occupation of defects level, e.g., two solid dots for a fully occupied defect level, one solid dot and one open dot for a half-occupied defect level, and two open dots for a fully unoccupied defect level.

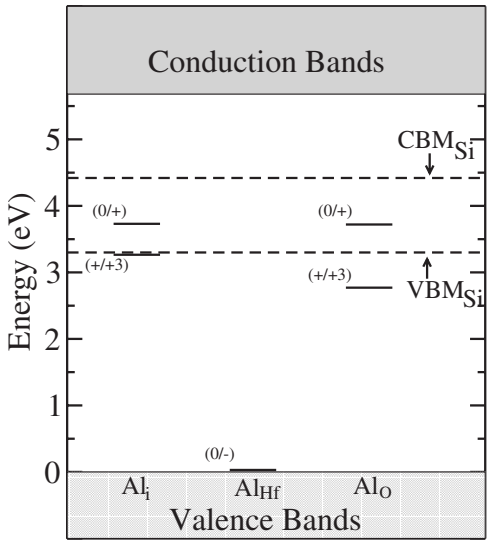

FIG. 5. The position of the thermodynamic transition energy levels in the experimental band gap (5.68 eV) of monoclinic HfO_2 for Al point defects. Conduction and valence band edges of silicon are also marked for references.

above the VBM induced by neutral Al_i is composed of a mixture of 3*p* orbitals of Al atom, 2*p* orbitals of neighboring oxygen atoms, and 5*d* orbitals of neighboring Hf atoms. The second highest defect level at 3.72 eV above the VBM due to neutral Al_i mainly comes from the 5*d* orbitals of Hf atom around the interstitial Al atom. Neutral Al_O also introduces two extra levels appearing in the upper part of the band gap: the level at 2.55 eV above the VBM is occupied by two electrons and composed of a mixture of 3*p* orbitals of the substitutional Al atom and 5*d* orbitals of neighboring Hf atoms, while another at 3.72 eV above the VBM is occupied by only one electron and comes from 5*d* orbitals of neighboring Hf atoms around the substitutional Al atom. For neutral Al_{Hf}, it introduces one extra level at 0.093 eV above the VBM. This extra level due to neutral Al_{Hf} is half occupied and composed of 2*p* orbitals of neighboring oxygen atoms around the substitutional Al atom, coming from the valence bands. Therefore, our results indicate that both interstitial Al and substitution of Al for O induce deep levels inside the band gap of HfO_2, while substitution of Al for Hf introduces acceptorlike level in the vicinity of the VBM. Due to the acceptorlike level introduced by substitution of Al for Hf, this kind of Al point defect therefore would strongly interact with its neighboring oxygen vacancies, suggesting the addition of Al into HfO_2 could passivate the defect states of oxygen vacancies.[7]

The location of the defect levels with respect to the valence and conduction band edges determines whether these defects affect the conductivity of the system studied.[30] The thermodynamic transition energy levels of interstitial and substitutional Al point defects in HfO_2 are calculated by the formula[31]

$$E_\alpha(q/q') = [\Delta E_f(\alpha,q) - \Delta E_f(\alpha,q')]/(q' - q) \quad (5)$$

and aligned with respect to the conduction and valence band edges of HfO_2 and silicon, using the valence band offset of HfO_2 on Si of ~3.3 eV,[32–34] as shown in Fig. 5. It should be noted that due to the energy band gap underestimation in LDA and GGA calculations, the conduction band edge of HfO_2 in Fig. 5 is shifted rigidly by a simple scissor operator and according to the experimental band-gap of HfO_2. This rigid correction would affect the predicted positions of shallow donor levels with respect to the conduction band edge of HfO_2. The acceptor level $E(0/-1)$ of substitutional Al on Hf site can trap electrons injected from the top of the silicon valence band. The donor levels $E(0/+1)$ of substitutional Al on oxygen site and interstitial Al point defects lie within the silicon energy gap and can act as hole-killer center for *p*-type silicon.

IV. CONCLUSIONS

First-principles calculations are performed to study the structural relaxation, energetics, and electronic structures of Al point defects in monoclinic HfO_2. The calculated formation energies indicate that under the oxygen-rich conditions the doped Al atom prefers to substitute for Hf atom and suggest that the formation of HfAlO laminate would be thermodynamically favorable. Either interstitial Al or substitution of Al for O introduces two deep levels inside the band gap of HfO_2. In contrast, substitutional Al on Hf site creates one shallow level near the VBM of HfO_2, behaving like an acceptor.

ACKNOWLEDGMENTS

The authors thank S.-H. Wei for his critical comments. X.G.G. is partially supported by the NSF of China, the national program for the basic research and research project of Shanghai. Q.L. acknowledges the RGC grant under Project No. 402105. Z.F.H. would like to thank Shanghai Postdoctoral Science Foundation (Grant No. 05R214106) and National Natural Science Foundation of China (Grant No. 10674028) for financial support. The computation was performed at Shanghai Supercomputer Center and Supercomputer Center of Fudan University.

[1] J. Robertson, J. Vac. Sci. Technol. B **18**, 1785 (2000).
[2] G. D. Wilk, R. M. Wallace, and J. M. Anthony, J. Appl. Phys. **89**, 5243 (2001).
[3] W. J. Zhu, T. Tamagawa, M. Gibson, T. Furukawa, and T. P. Ma, IEEE Electron Device Lett. **23**, 649 (2002).
[4] H. Y. Yu, M. F. Li, B. J. Cho, C. C. Yeo, M. S. Joo, D.-L. Kwong, J. S. Pan, C. H. Ang, J. Z. Zheng, and S. Ramanathan, Appl. Phys. Lett. **81**, 376 (2002).
[5] S. H. Bae, C. H. Lee, R. Clark, and D. L. Kwong, IEEE Electron Device Lett. **24**, 556 (2003).
[6] S. Zafar, A. Kumar, E. Gusev, and E. Cartier, IEEE Trans. Device Mater. Reliab. **5**, 45 (2005).
[7] Q. Li, K. M. Koo, W. M. Lau, P. F. Lee, J. Y. Dai, Z. F. Hou, and X. G. Gong, Appl. Phys. Lett. **88**, 182903 (2006).
[8] Y. G. Fedorenko, V. V. Afanas'ev, and A. Stesmans, Microelectron. Eng. **80**, 66 (2005).
[9] G. Kresse and J. Furthmüller, Comput. Mater. Sci. **6**, 15 (1996).
[10] G. Kresse and J. Furthmüller, Phys. Rev. B **54**, 11169 (1996).
[11] J. P. Perdew, J. A. Chevary, S. H. Vosko, K. A. Jackson, M. R. Pederson, D. J. Singh, and C. Fiolhais, Phys. Rev. B **46**, 6671 (1992).
[12] D. Vanderbilt, Phys. Rev. B **41**, 7892 (1990).
[13] G. Kresse and J. Hafner, J. Phys.: Condens. Matter **6**, 8245 (1994).
[14] H. J. Monkhorst and J. D. Pack, Phys. Rev. B **13**, 5188 (1976).
[15] J. Wang, H. P. Li, and R. Stevens, J. Mater. Sci. **27**, 5397 (1992).
[16] D. M. Adams, S. Leonard, D. R. Russel, and R. J. Cernik, J. Phys. Chem.

Solids **52**, 1181 (1991).
[17]D. W. Stacy, J. K. Johnstone, and D. R. Wilder, J. Am. Ceram. Soc. **55**, 482 (1972).
[18]A. S. Foster, F. L. Gejo, A. L. Shluger, and R. M. Nieminen, Phys. Rev. B **65**, 174117 (2002).
[19]J. Kang, E.-C. Lee, and K. J. Chang, Phys. Rev. B **68**, 054106 (2003).
[20]D. R. Lide, *CRC Handbook of Chemistry and Physics* (CRC, New York, 1998).
[21]C. Kittel, *Introduction to Solid State Physics*, 6th ed. (Wiley, New York, 1986).
[22]H. d'Amour, D. Schiferl, W. Denner, H. Schulz, and W. B. Holzafet, J. Appl. Phys. **49**, 4411 (1978).
[23]K. Matsunaga, T. Tanaka, T. Yamamoto, and Y. Ikuhara, Phys. Rev. B **68**, 085110 (2003).
[24]H. S. Chang, H. S. Hwang, M.-H. Cho, S. J. Doh, J. L. Lee, and N.-I. Lee, Appl. Phys. Lett. **84**, 28 (2004).
[25]S. B. Zhang and J. E. Northrup, Phys. Rev. Lett. **67**, 2339 (1991).
[26]S.-H. Wei, Comput. Mater. Sci. **30**, 337 (2004).
[27]C. G. Van de Walle and J. Neugebauer, J. Appl. Phys. **95**, 3851 (2004).
[28]D. B. Laks, C. G. Van de Walle, G. F. Neumark, P. E. Blöhl, and S. T. Pantelides, Phys. Rev. B **45**, 10965 (1992).
[29]W. L. Scopel, A. J. R. da Silva, W. Orellana, and A. Fazzio, Appl. Phys. Lett. **84**, 1492 (2004).
[30]J. M. Pruneda and E. Artacho, Phys. Rev. B **71**, 094113 (2005).
[31]S. B. Zhang, S.-H. Wei, and A. Zunger, Phys. Rev. B **63**, 075205 (2001).
[32]S. Sayan, E. Garfunkel, and S. Suzer, Appl. Phys. Lett. **80**, 2135 (2002).
[33]P. W. Peacock and J. Robertson, J. Appl. Phys. **92**, 4712 (2002).
[34]M. Oshima, S. Toyoda, T. Okumura, J. Okabayashi, H. Kumigashira, K. Ono, M. Niwa, K. Usuda, and N. Hirashita, Appl. Phys. Lett. **83**, 2172 (2003).